2012

Sound Attenuation in Elliptic Mufflers Using a Regular Perturbation Method

Subhabrata Banerjee
banerje6@illinois.edu

Anthony M. Jacobi

Sound Attenuation in Elliptic Mufflers Using a Regular Perturbation Method

Subhabrata Banerjee[1], Anthony M. Jacobi*[1]

[1]Department of Mechanical Science and Engineering,
University of Illinois at Urbana-Champaign,
Urbana, IL, USA.
banerje6@illinois.edu, a-jacobi@illinois.edu

* Corresponding Author

ABSTRACT

The study of sound attenuation in an elliptical chamber involves the solution of the Helmholtz equation in elliptic coordinate systems. The Eigen solutions for such problems involve the Mathieu and the modified Mathieu functions. The computation of such functions poses considerable challenge. An alternative method to solve such problems had been proposed in this paper. The elliptical cross-section of the muffler has been treated as a perturbed circle, enabling the use of a regular perturbation approach to solve the wave equation. The Eigen vectors of the perturbed system has been approximated by a series summation of the unperturbed Eigen solutions. The acoustic pressure in the elliptical duct has been derived from the perturbed Eigen vectors by using the Green's function approach.

1. INTRODUCTION

Ducts having hollow or annular elliptic cross-sections are widely used in automotive systems and in hermetic compressors to attenuate sound. Therefore, studying the propagation of sound in such ducts is important from a design perspective. Unlike circular or rectangular chamber mufflers, study on elliptical geometries (either analytically or numerically) has not been widely reported in literature. The effect of geometry has an important effect on the three-dimensional propagation, since higher order modes can be suppressed by proper choice of geometry and location of the inlet/outlet. Moreover, the cross-section influences the shape of the resonant peaks in acoustically short chamber mufflers (Ih and Lee, 1985). This highlights the importance in studying elliptical mufflers. The effects of eccentricity on the cutoff frequency for the higher order circumferential mode for an elliptic duct was studied by Lawson (1975). Hong *et al.* (1995) calculated the natural frequencies and studied the mode shapes for hollow and annular elliptic chambers. Comparisons were made to equivalent circular geometries. Denia *et al.* (2001) studied the attenuation characteristics of elliptic mufflers for various lengths and eccentricities using a truncated mode superposition technique similar to that reported by Kim *et al.* (1989).They solved for the Helmholtz equation in an elliptic domain, the solution (Eigen functions) was expressed in terms of Mathieu and modified Mathieu functions and the four-pole parameters were derived from them. Selamet *et al.* (2001) used the finite element method (FEM) to find the attenuation characteristics of short elliptic chamber mufflers with center inlet and side outlet configurations. The analytical solution to the center inlet and side outlet short elliptical muffler was later reported by Banerjee *et al.* (2011) and Mimani *et al.* (2011) and agreed well with the FEM and experimental results.

The computation of Mathieu or modified Mathieu functions poses considerable computation effort. This makes analysis of elliptical mufflers time consuming. A possible way for avoiding such tedious computation is by approximating the ellipse by a perturbed circle. Such approach has been reported by Nayfeh *et al.* (1975) in determining the natural frequencies and mode shapes of vibrating elliptical plates. In this method, the ellipse is approximated by a circle with a small perturbation. The governing Eigen value problem is solved by approximating

the solutions as a series summation of the Eigen vectors of a circle having equivalent radius as the ellipse. The boundary conditions are imposed after transferring them from the elliptical surface to the perturbed surface. The method works when the eccentricity of the ellipse is small. To our knowledge, such methods have not been implemented for an elliptical muffler to determine its sound attenuation. The present work is aimed at finding the TL in an elliptical muffler using a regular perturbation method outlined by Nayfeh *et al.* (1973, 1975). A Green's function is defined using the perturbed Eigen vectors. Finally, a Green's function based method similar to (Kim *et al.*,1993, Venkatesham *et al.*,2009, Banerjee *et al.*,2011, Mimani *et al.*,2011) is implemented obtain the TL.

2. MATHEMATICAL FORMULATION

The linear wave equation in terms of the velocity potential in three dimensional space is given as:

$$\nabla^2\phi(\vec{x}) + k^2\phi(\vec{x}) = 0 \tag{1}$$

where, k is the wave number. For an elliptical duct $\vec{x} = (\xi, \eta, z)$, $0 \le \xi \le \xi_0$, $0 \le \eta \le 2\pi$, $0 \le z \le L$.

The Eigen solution to the above problem for a duct having an elliptical cross section will involve Mathieu and modified Mathieu functions. In order to avoid the complexity in computing these functions, the elliptical geometry is approximated as a perturbed circular cylinder. The geometry of the perturbed cylinder can be obtained as follows:

The equation of an ellipse is given by:

$$\left(\frac{x}{a}\right)^2 + \left(\frac{y}{b}\right)^2 = 1 \tag{2}$$

Where a and b are the semi-major axis and semi-minor axis of the ellipse, respectively. The eccentricity of the ellipse is given by $e = \sqrt{1-(b/a)^2} = \sec h\xi_0$. The semi-interfocal distance of the ellipse is given by $h = ae$.

$$\text{Let } x = r\cos\theta,\ y = r\sin\theta \tag{3}$$

Substituting Eqn. (3) into Eqn. (2), yields

$$r = \frac{a}{\sqrt{1 + \frac{e^2}{2(1-e^2)}(1-\cos(2\theta))}} \tag{4}$$

For small eccentricities, the denominator of Eqn. (4) can be expanded in an infinite series. Collecting terms of each order of $\cos\theta$, r can simplified as:

$$r \simeq a\left[1 - \frac{e^2}{4} + \frac{9e^4}{64}\right] + a\left[\frac{e^2}{4} - \frac{3e^4}{16}\right]\cos(2\theta) + O(e^4) \tag{5}$$

In a compact form, r can be written as:

$$r = R + \varepsilon f(\theta) + O(\varepsilon^2) \tag{6}$$

where,

$$R = a\left[1 - \frac{e^2}{4} + \frac{9e^4}{64}\right],\ \varepsilon = a\left[\frac{e^2}{4} - \frac{3e^4}{16}\right],\ f(\theta) = \cos(2\theta) \tag{7}$$

In the present analysis, the muffler is assumed to be rigid. Therefore, the normal component of the velocity at the boundaries should be zero:

$$\left.\frac{\partial\phi}{\partial r}\right|_{r=R+\varepsilon f(\theta)} = 0,\ \left.\frac{\partial\phi}{\partial z}\right|_{z=0,L} = 0 \tag{8}$$

Expanding Eqn. (8) in a Taylor series leads to:

$$\left.\frac{\partial\phi}{\partial r}\right|_{r=R+\varepsilon f(\theta)} = \left.\frac{\partial\phi}{\partial r}\right|_{r=R} + \varepsilon f(\theta)\left.\frac{\partial^2\phi}{\partial r^2}\right|_{r=R} + ... = 0 \tag{9}$$

We assume that the Eigen functions and the Eigen values can be expanded (Nayfeh *et al*., 1975) according to:

$$\begin{aligned}\phi(r,\theta;\varepsilon) &= \phi_0(r,\theta) + \varepsilon\phi_1(r,\theta) + \varepsilon^2\phi_2(r,\theta) + ... \\ k(\varepsilon) &= k_0(\varepsilon) + \varepsilon k_1(\varepsilon) + \varepsilon^2 k_2(\varepsilon) + ...\end{aligned} \tag{10}$$

Substituting Eqn. (10) into Eqns. (1) and (8) and collecting terms of each order of ε leads to the following sets of problem:

Order ε^0:

$$\begin{aligned}&\nabla^2\phi_0 + k_0^2\phi_0 = 0 \\ &\left.\frac{\partial\phi_0}{\partial r}\right|_{r=R} = 0,\ \left.\frac{\partial\phi_0}{\partial z}\right|_{z=0,L} = 0\end{aligned} \tag{11}$$

Where $\nabla^2 = \frac{\partial^2}{\partial r^2} + \frac{1}{r}\frac{\partial}{\partial r} + \frac{1}{r^2}\frac{\partial^2}{\partial\theta^2} + \frac{\partial^2}{\partial z^2}$

Order ε^1:

$$\begin{aligned}&\nabla^2\phi_1 + 2k_0k_1\phi_0 + k_0^2\phi_1 = 0 \\ &\left\{\frac{\partial\phi_1}{\partial r} + f(\theta)\frac{\partial^2\phi_0}{\partial r^2}\right\}_{r=R} = 0,\ \left.\frac{\partial\phi_1}{\partial z}\right|_{z=0,L} = 0\end{aligned} \tag{12}$$

The general solution to Eqn. (11) is given by:

$$\begin{aligned}&\phi_0 = \sum_{n=0}^{\infty}\sum_{m=1}^{\infty}\sum_{p=0}^{\infty}\left(A_{nm}e^{in\theta} + \bar{A}_{nm}e^{-in\theta}\right)J_n(k_{0rnm}r)\cos(\frac{p\pi}{L}z) \\ &\text{where} \\ &\left.\frac{dJ_n(k_{0rnm}r)}{dr}\right|_{r=R} = 0\end{aligned} \tag{13}$$

k_{0rnm} are an infinite number of roots corresponding to each order *n* of the derivative of the Bessel function. The eigenvalue k_{0nm} corresponding to each mode (*n*, *m*, *p*) is related to k_{0rnm} through the following relation:

$$k_{0rnm} = \sqrt{k_{0nm}^2 - \left(\frac{p\pi}{L}\right)^2},\quad n = 0,1,2,.....\quad m = 1,2,3,.....\quad p = 0,1,2,..... \tag{14}$$

The correction to one of the terms in Eqn. (11) is obtained by substituting one of the modes in Eqn. (13) into Eqn. (12), which leads to:

$$\nabla^2\phi_1 + k_{0nm}^2\phi_1 = -2k_{0nm}k_1J_n(k_{0rnm}r)\left(A_{nm}e^{in\theta} + \bar{A}_{nm}e^{-in\theta}\right)\cos(\frac{p\pi}{L}z) \tag{15}$$

Expanding ϕ_1, $f(\theta)$ in Fourier series leads to:

$$\phi_1 = \sum_{s=0}^{\infty}\beta_s(r)\left(B_se^{is\theta} + \bar{B}_se^{-is\theta}\right)\cos(\frac{p\pi}{L}z) \tag{16}$$

$$f(\theta) = \sum_{q=1}^{\infty}\left(f_qe^{iq\theta} + \bar{f}_qe^{-iq\theta}\right) \tag{17}$$

Substituting Eqn. (16) and Eqn. (17) into Eqn. (15), multiplying both sides of Eqn. (15) by $e^{-ik\theta}$ and integrating w.r.t θ from 0 to 2π yields (Nayfeh *et al*., 1975):

$$\left(\frac{\partial^2}{\partial r^2}+\frac{1}{r}\frac{\partial}{\partial r}-\frac{k^2}{r^2}+k_{0rnm}\right)\beta_k=\begin{cases}-2k_{0nm}k_1\dfrac{A_{nm}}{B_n}J_n(k_{0rnm}r) & k=n\\ 0 & k\neq n\end{cases} \tag{18}$$

$$\beta_k'(R)=-\frac{1}{B_k}J_n^*(k_{0rnm}R)\begin{cases}\bar{A}_{nm}f_{n+k}+A_{nm}f_{n-k} & k<n\\ \bar{A}_{nm}f_{2n} & k=n\neq 0\\ \bar{A}_{nm}f_{n+k}+A_{nm}f_{k-n} & k>n\end{cases}$$

For $k\neq n$, the solution to Eqn. (18) is $\beta_k=\alpha_1 J_k(k_{0rnm}r)$, where the coefficient α_1 is determined from the boundary conditions:

$$\alpha_1=-\frac{1}{B_k}\frac{J_n^*(k_{0rnm}r)}{J_n'(k_{0rnm}r)}\bigg|_{r=R}\begin{cases}\bar{A}_{nm}f_{n+k}+A_{nm}f_{n-k} & k<n\\ \bar{A}_{nm}f_{n+k}+A_{nm}f_{k-n} & k>n\end{cases} \tag{19}$$

When $k=n$, multiplying both sides of Eqn. (18) and integrating w.r.t *r* results:

$$\int_0^R\left[\left(\frac{\partial^2}{\partial r^2}+\frac{1}{r}\frac{\partial}{\partial r}-\frac{n^2}{r^2}+k_{0rnm}\right)\beta_n\right]rJ_n(k_{0rnm}r)dr=-\int_0^R 2k_{0nm}k_1\frac{A_{nm}}{B_n}J_{nm}^2(k_{0rnm}r)rdr \tag{20}$$

Integrating by parts and substituting the boundary condition, k_1 is derived as:

$$k_1=\frac{\bar{A}_{nm}rJ_n^*(k_{0rnm}r)J_n(k_{0rnm}r)f_{2n}}{2k_{0nm}A_{nm}\int_0^R J_n^2(k_{0rnm}r)rdr}\bigg|_{r=R}=\frac{\bar{A}_{nm}}{A_{nm}}S,\quad\text{where } S=\frac{rJ_n^*(k_{0rnm}r)J_n(k_{0rnm}r)f_{2n}}{2k_{0nm}\int_0^R J_n^2(k_{0rnm}r)rdr}\bigg|_{r=R} \tag{21}$$

From the condition that k_1 should be real:

$$\bar{A}_{nm}/A_{nm}=\pm 1 \tag{22}$$

Therefore, for each (*n, m, p*), there are two Eigen values and two Eigen functions. Having determined k_1, β_n can be determined as follows:

$$\text{Let } \beta_n(r)=\beta_n^h(r)+\beta_n^p(r) \tag{23}$$

The superscripts *h* and *p* indicate the homogeneous solution and the particular integral, respectively. The homogeneous solution is given by $\beta_n^h(r)=\alpha_n J_n(k_{0nm}r)$. The particular solution can be derived in a way similar to that given by Nayfeh *et al.* (1975). For the present problem the particular integral has been taken as zero. This results in some error because then the Eqn. (18) is not satisfied for *n > 0*. However, the error is observed to be marginal and does not justify the computational effort.

The final form of the velocity potential up to $O(\varepsilon)$ can be expressed as:

$$\phi_{n,m,p}^{(1)}\sim A_{nm}\left[J_n(k_{0rnm}r)\cos(n\theta)+\varepsilon\sum_{s=0}^{\infty}-\frac{J_n^*(k_{0rnm}r)}{J_n'(k_{0rnm}r)}\bigg|_{r=R}\left(f_{n+s}+\bar{f}_{n-s}\right)J_s(k_{0rnm}r)\cos(s\theta)\right]\cos\left(\frac{p\pi}{L}z\right);\quad\begin{matrix}n=0,1,....\\ m=1,2,....\\ p=0,1,....\end{matrix}$$

$$k_{nmp}^{(1)}=\sqrt{k_{0rnm}^2+\left(\frac{p\pi}{L}\right)^2}+\varepsilon S \tag{24}$$

$$\phi^{(2)}_{n,m,p} \sim B_{nm}\left[J_n(k_{0rnm}r)\sin(n\theta) + \varepsilon\sum_{s=1}^{\infty} -\frac{J_n^{'}(k_{0rnm}r)}{J_n^{'}(k_{0rnm}r)}\bigg|_{r=R} \left(f_{n+s} + \overline{f}_{n-s} \right) J_s(k_{0rnm}r)\sin(s\theta) \right] \cos(\frac{p\pi}{L}z); \quad \begin{matrix} n = 1,2,,.... \\ m = 1,2,.... \\ p = 0,1,.... \end{matrix} \tag{25}$$

$$k^{(2)}_{nmp} = \sqrt{k^2_{0rnm} + \left(\frac{p\pi}{L}\right)^2} - \varepsilon S$$

where, S is given by Eqn. (21)

3. DETERMINATION OF THE TRANSMISSION LOSS

A Green's function based approach outlined by Kim *et al.* (1993) has been implemented to calculate the pressure distribution in the muffler. The Green's function satisfies the Helmholtz equation in the domain defined by Eqn. (1)

$$\nabla^2 G(\vec{r} / \vec{r}_o) + k^2 G(\vec{r} / \vec{r}_o) = -\delta(\vec{r} - \vec{r}_o) \tag{26}$$

Here $\vec{r} = (\eta, \xi, z)$ and $\vec{r}_o = (\eta_o, \xi_o, z_o)$ are the coordinates of the source and the observer respectively. The Green's function satisfies the homogeneous boundary condition over the surface.

The Green's function for the elliptical problem can be expressed as a series of the Eigen functions:

$$G(\vec{r} / \vec{r}_o) = \sum_{n=0}^{\infty}\sum_{m=1}^{\infty}\sum_{p=0}^{\infty} \frac{\phi^{(1)}_{n,m,p}(\vec{r})\phi^{(1)}_{n,m,p}(\vec{r}_0)}{\left(\left[k^{(1)}_{nmp}\right]^2 - k^2\right)\int_V \left[\phi^{(1)}_{n,m,p}(\vec{r})\right]^2 dV} + \sum_{n=1}^{\infty}\sum_{m=1}^{\infty}\sum_{p=0}^{\infty} \frac{\phi^{(2)}_{n,m,p}(\vec{r})\phi^{(2)}_{n,m,p}(\vec{r}_0)}{\left(\left[k^{(2)}_{nmp}\right]^2 - k^2\right)\int_V \left[\phi^{(2)}_{n,m,p}(\vec{r})\right]^2 dV} \tag{27}$$

For the muffler, the inlet and outlet are assumed to be uniform velocity piston sources. The solution to the homogeneous Eqn. (1) with inhomogeneous boundary conditions (piston sources) can be derived using the reciprocity relation of the Green's function and by using Green's second identity:

$$\begin{aligned} \phi(\vec{r}) &= \int_{S_0} G(\vec{r} / \vec{r}_0)\nabla\phi(\vec{r}_0)\cdot dS_0 \\ &\sim \int_{Inlet\ Piston} G(\vec{r} / \vec{r}_0)\nabla\phi(\vec{r}_0)\cdot d\vec{S}_0 + \int_{Outlet\ Piston} G(\vec{r} / \vec{r}_0)\nabla\phi(\vec{r}_0)\cdot d\vec{S}_0 \end{aligned} \tag{28}$$

Since, a uniform velocity piston source was assumed at the inlet and at the outlet with inlet velocity u_1 and outlet velocity u_2, therefore $\nabla\phi(\vec{r}_0)\cdot d\vec{S}_0 = -u_1 dS_0$ and $\nabla\phi(\vec{r}_0)\cdot d\vec{S}_0 = u_2 dS_0$ at the inlet and outlet, respectively.

Having found the velocity potential, the average sound pressure acting on the piston '*i*' with cross-section area S_i is derived as (Ih and Lee, 1987):

$$P_i = -\frac{j\rho\omega}{S_i}\int_{S_i} \phi(\vec{r}) dS_i \tag{29}$$

If we denote the inlet and the outlet pistons by '1' and '2' respectively, then Eqn. (29) can be derived in the form (Ih and Lee, 1987):

$$\begin{aligned} P_1 &= -jU_1 Z_o E_{11} + jU_2 Z_o E_{12} \\ P_2 &= jU_2 Z_o E_{22} - jU_1 Z_o E_{21} \end{aligned} \tag{30}$$

The functions: $E_{ij} : i, j = 1,2$ are derived from Eqn. (28) and Eqn. (29) and they depend on the geometry of the muffler as well as the location of the inlet and the outlet ports. $Z_0 = \rho c / S$ is the characteristic impedance of the chamber, S is the area of cross-section of the chamber. U_1 and U_2 are the volume velocities at the inlet and outlet,

respectively. The upstream and the downstream pressure and velocity can be rearranged in the following form (Munjal, 1987):

$$\begin{Bmatrix} P_1 \\ U_1 \end{Bmatrix} = \begin{bmatrix} T_{11} & T_{12} \\ T_{21} & T_{22} \end{bmatrix} \begin{Bmatrix} P_2 \\ U_2 \end{Bmatrix} \tag{31}$$

Finally the TL in the muffler is expressed as (Munjal, 1987):

$$TL = 20\log_{10}\left\{\frac{1}{2}\left(\frac{Z_2}{Z_1}\right)^{1/2}\left|T_{11} + T_{12}/Z_2 + T_{21}Z_1 + T_{22}(Z_1/Z_2)\right|\right\} \tag{32}$$

$Z_1 = \rho c / S_1$ and $Z_2 = \rho c / S_2$ are the characteristic impedances of the inlet and the outlet, respectively. S_1 and S_2 are the area of cross-section of the inlet and the outlet piston.

4. RESULTS AND DISCUSSIONS

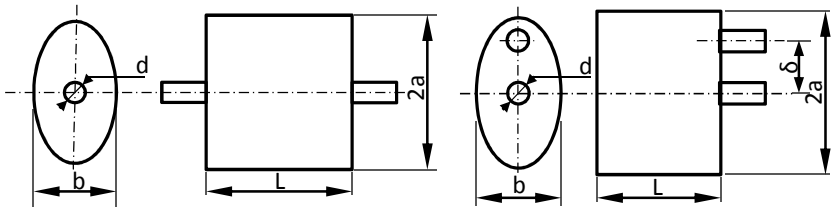

(a) (b)

Figure 1: Schematic diagram of the elliptical mufflers with different inlet/outlet configurations: (a) Concentric chamber muffler (b) Reversing chamber muffler with inlet at the center and outlet on the major axis.

The TL and the natural frequencies corresponding to various modes as determined by the perturbation method were compared to the results given by Denia *et al.* (2001). Two different muffler configurations have been considered for the comparison: (i) Concentric chamber mufflers (ii) Reversing chamber mufflers. The geometries of the mufflers shown in fig.2 are same as those given by Denia *et al.* (2001). The details of the dimensions are presented in table 1.

Table 2 presents the comparison of the natural frequencies of various modes obtained by analytical (Denia *et al.*, 2001) and by the perturbation method. For reference, the natural frequency of a circular muffler having same area of cross section as the ellipse is also presented. It can be observed from the table that the perturbation method predicts a lower values of the frequency corresponding to the (*n*, *m*>1) mode. It is proposed that while using the perturbation method in the large eccentricity limit, only modes of the type (*n*, 1) should be considered for calculating the TL. From the table 2, the analytically calculated frequency corresponding to the (0, 2) mode is 2840.89 Hz. The perturbation method predicts the (0, 2) mode frequency as 1999. 85 Hz. Therefore, the perturbation problem predicts the propagation of the (0, 2) modes at a much lower frequency than the actual (analytical) frequency. This lead to significant differences between the analytical and the perturbation TL curves beyond the predicted (0, 2) mode frequency (fig. 2). However, if the (*n*, *m*>1) modes are neglected, the TL curves show very good agreement except for minor differences due to different cross- section areas. The agreement is up to the theoretical value of the frequency corresponding to the (0, 2) mode, beyond which the curves diverge. For most muffler geometries, the (0, 2) mode propagate at fairly large frequency. Therefore, the suppression of the (*n*, *m*>1) modes can be applied for determining the TL over a wide frequency range without affecting the accuracy of the solution in a significant way. In an acoustically short chamber, the higher order modes are not completely decayed in an axial direction. These higher order evanescent modes affect the TL even below their cutoff frequency (Ih and Lee, 1987). Neglecting the

(n, m>1) modes in such mufflers results in an erroneous TL curve even in the low frequency region. Therefore, the suppression of the higher order modes is valid for acoustically long mufflers only.

Table 1

Details of the muffler dimensions

Orientation	a (m)	b (m)	L (m)	r (m)	δ (m)	ε
Concentric	0.23/2	0.13/2	0.25	0.033/2	----	0.82
Reversing	0.23/2	0.13/2	0.35	0.033/2	0.06	0.82

Table 2

Comparison of natural frequencies for different even modes
(a *= 0.23/2 m,* b *= 0.13/2 m*)

Mode	Denia *et al*., 2001	Perturbation method	Equivalent Circle
(0,1)	0.0	0.0	0.0
(0,2)	2840.89	1999.85	2399.30
(0,3)	5469.52	3658.93	4392.68
(1,1)	880.00	900.57	1152.87
(1,2)	3375.98	2607.68	3382.64
(1,3)	5988.36	4175.14	5344.87
(2,1)	1599.21	1592.78	1912.20
(2,2)	3946.36	3497.50	4198.89
(2,3)	6525.74	5199.47	6242.16
(3,1)	2297.99	2191.06	2630.45
(2,2)	4547.05	4180.03	5018.56
(3,3)	7079.83	5917.35	7104.00
(4,1)	2982.86	2773.15	3329.31
(4,2)	5173.36	4841.11	5811.94
(4,3)	7649.01	6614.08	7940.45

Figure 2 shows the TL curves for the concentric chamber muffler obtained by the perturbation method. The TL from the analytical results and from an equivalent circle is also plotted. The suppression of the higher order modes significantly improves the perturbation result. Below the frequency corresponding to the (2, 1) mode, all the curves predict the dome like TL curve usually observed for plane wave propagation. The magnitude of the TL depends on the area ratio of inlet to the chamber. The area of the perturbed circle is larger than the ellipse or the equivalent circle. This explains a higher TL prediction for the perturbed geometry. At about 1600 Hz, the (2, 1) mode in the ellipse propagates, which results in a collapse in the TL curve. The perturbed geometry is able to predict this behavior and shows very good agreement to the analytical result. For a concentric circular chamber, the (2, 1) mode is not active. Therefore, the equivalent circle approach fails to predict the TL beyond the frequency corresponding to (2, 1) mode. At about 2400 Hz, the (0, 2) mode for the circle is active, which results in a decay in TL. The (0, 2) mode for the ellipse is at about 2800 Hz. Therefore, the TL curve for the ellipse starts to decay later than the circle. The perturbed method begins to differ from the analytical solution near the (0, 2) mode as expected.

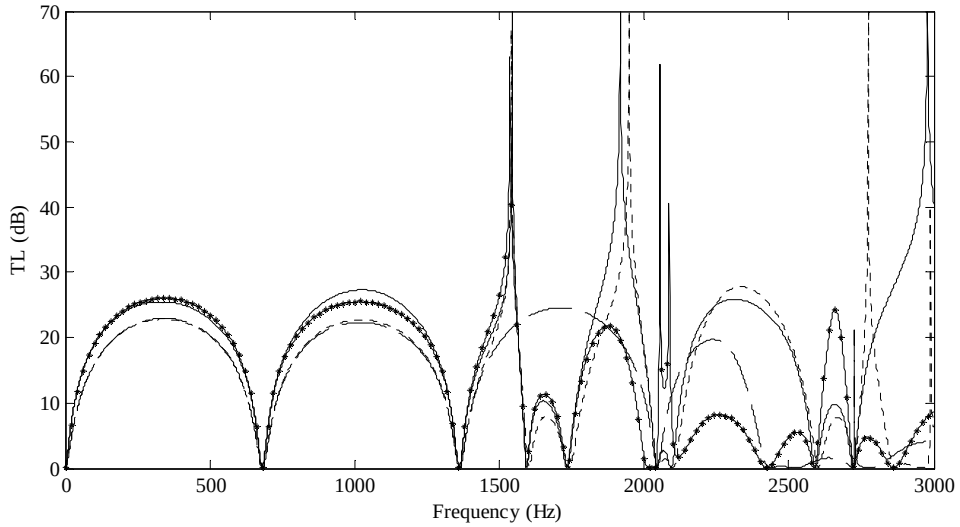

Figure 2: TL for a concentric chamber muffler with length, L = 0.25 m: _____, perturbation solution (R = 0.103 m, ε = 0.0095); ..... , analytical method (a = 0.23/2 m, b = 0.13/2 m) (Denia *et al.*, 2001); _ _ _ , equivalent circular chamber (R = 0.0864 m); -*-*-*-*, perturbation solution with higher order mode effects (R = 0.103 m, ε = 0.0095)

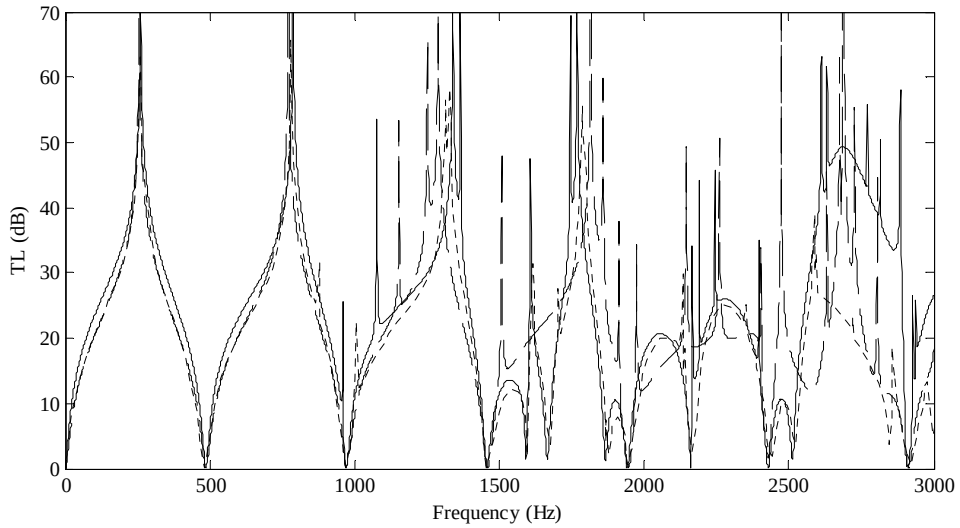

Figure 3: TL for a reversing chamber muffler with length, L = 0.35 m: _____, perturbation solution (R = 0.103 m, ε = 0.0095); ..... , analytical method (a = 0.23/2 m, b = 0.13/2 m) (Denia *et al.*, 2001); _ _ _ , equivalent circular chamber (R = 0.0864 m).

Figure 3 shows the comparison of the TL curves for a reversing chamber muffler with length, L = 0.35 m. The perturbation results are in good agreement with the analytical result below the (0, 2) cutoff frequency. The equivalent circular chamber fails to predict the TL beyond the (2, 1) mode.

6. CONCLUDING REMARKS

The TL in elliptic chamber mufflers was developed using a regular perturbation approach. The elliptical geometry was approximated by a perturbed circle and the governing wave equation was solved by transferring the boundary

condition from the ellipse to the perturbed boundary. A Green's function based method was implemented to find the TL. The frequency of the (n, m>1) modes showed significant departure from the analytical values. This led to a deviation in the approximate TL curve from the analytical curve. The suppression of the (n, m>1) greatly improved the frequency range up to the analytical value of the propagation of the (0, 2) mode for acoustically short mufflers. The agreement between the analytical and the perturbation solution proved the effectiveness of the perturbation method over a wide frequency range.

REFERENCES

Banerjee, S., Jacobi, A.M., 2011, Analysis of sound attenuation in elliptical chamber mufflers by using Green's function, *Proc. of the ASME 2011 International Mechanical Engineering Congress & Expositions, Denver, USA.*

Denia, F.D., Albelda, J., Fuenmayor, F.J., 2001, Acoustic behavior of elliptical chamber mufflers, *J. Sound and Vib.*, vol. 241: p. 401–421.

Hong, K., Kim, J., 1995, Natural mode analysis of hollow and annular elliptical cylindrical cavities, *J. Sound and Vib.*, vol. 183: p. 327–351.

Ih, J.G., Lee, B.H., 1985, Analysis of higher order mode effects in the circular expansion chamber with mean flow. *J. Acoust. Soc. of America*, vol. 77: p. 1377-1388.

Kim, J., Seodel, W., 1989, General formulation of four pole parameters for three-dimensional cavities utilizing modal expansion, with special attention to the annular cylinder, *J. Sound and Vib.*, vol. 129: p. 237-254.

Kim, Y.H., Kang, S.W., 1993, Green's solution of the acoustic wave equation for a circular expansion chamber with arbitrary locations of inlet, outlet port, and termination impedance, *J. Acoust. Soc. of America*, vol. 94: p. 473–490.

Lawson, M.V., Baskaran, S., 1975, Propagation of sound in elliptic ducts, *J. Sound and Vib.*, vol. 38: p. 185–194.

Mimani, A., Munjal, M.L., 2011, 3-D acoustic analysis of elliptical chamber mufflers having an end-inlet and a side-outlet: An impedance matrix approach, *Wave Motion*, vol. 49: p. 271-295.

Munjal, M.L., 1987, *Acoustics of Ducts and Mufflers*, Wiley, New York.

Nayfeh, A. H., 1973, *Perturbation methods*, Wiley-Interscience, New-York.

Nayfeh, A. H., Mook, D.T., Lobitz, D.W., Sridhar, S., 1975,Vibration of nearly annular and circular plates, *J. Sound and Vib.*, vol. 47: p.75-84.

Selamet, A., Denia, F.D., 2001, Acoustic behavior of short elliptical chambers with end central inlet and end offset or side outlet, *J. Sound and Vib.*, vol. 245: p. 953–959.

Venkatesham, B., Tiwari, M., Munjal, M.L., 2009, TL analysis of rectangular expansion chamber muffler with arbitrary location of inlet/outlet by means of Green's function, *J. Sound and Vib.*, vol. 323: p. 1032–1044.

ACKNOWLEDGEMENT

The authors would like to thank the Air-conditioning and Refrigeration Center (ACRC) at the University of Illinois, Urbana-Champaign for providing the required resources for the research work reported here.